Makara J. Technol. 23/2 (2019), 53-58
doi: 10.7454/mst.v23i2.3634

A Study of the Electron Regeneration Efficiency of Solar Cells Fabricated Using CMC/PVA-, Alginate-, and Xanthan-based Electrolytes

Nur Farha Shaafi[1], Saifful Kamaluddin Muzakir[1*], and Bouchta Sahraoui[2]

1. Material Technology Program, Faculty of Industrial Sciences & Technology, Universiti Malaysia Pahang, Lebuhraya Tun Razak, Gambang 26300, Kuantan, Pahang, Malaysia
2. University of Angers, UFR Sciences, Institute of Sciences and Molecular Technologies of Angers MOLTECH Anjou-UMR CNRS 6200, 2 Bd Lavoisier 49045 ANGERS Cedex 2, France

[*]*e-mail: saifful@ump.edu.my*

Abstract

A photovoltaic (PV) mechanism consists of three important steps, i.e., (i) electron excitation upon absorption of photon with energy higher than the bandgap of fluorophore, (ii) excited-state electron injection from the fluorophore to the photoelectrode, and (iii) electron regeneration from the electrolyte to the fluorophore. An efficient electron regeneration could be achieved upon fulfillment of the requirements of energy alignment, i.e., lowest unoccupied molecular orbital of fluorophore ($LUMO_{fluorophore}$) > redox potential of electrolyte > highest occupied molecular orbital of fluorophore ($HOMO_{fluorophore}$). This study investigated the electron regeneration efficiency of excitonic solar cells fabricated using three polymer-based electrolytes, i.e., (i) 60% carboxymethyl cellulose (CMC) blended with 40% polyvinyl alcohol (PVA), (ii) alginate, and (iii) xanthan. The redox potentials of the electrolytes (E_o) were calculated using quantum chemical calculations under the framework of density functional theory. The compatibility of fluorophore and electrolyte was analyzed in terms of the energy level alignment. The cells fabricated using the three polymer-based electrolytes were analyzed, with the CMC/PVA-based cell yielding the highest efficiency, η, of 1.39% under the illumination of the sun. The low η of the cells can be attributed to the incompatible E_o of the electrolytes, which exhibited a higher energy level than the $LUMO_{fluorophore}$. The alginate- and xanthan-based cells exhibited inferior PV properties (i.e., open circuit voltage, short circuit current, fill factor, and η) to that of the CMC/PVA-based cell. This finding can be attributed to the increment of energy offset between E_o and $HOMO_{fluorophore}$.

Abstract

Sebuah Studi Tentang Efisiensi Regenerasi Elektron Sel Surya yang Dibuat Menggunakan CMC/PVA-, Alginat-, dan Elektrolit Berbasis Xanthan. Mekanisma fotovoltaik (PV) terdiri daripada tiga langkah penting iaitu (i) pengujaan elektron apabila penyerapan foton dengan tenaga yang lebih tinggi daripada jurang jalur fluorofora, (ii) suntikan elektron yang teruja dari fluorofora kepada fotoelektrod, dan (iii) pengenerasian semula elektron daripada elektrolit ke fluorofora. Pengenerasian semula elektron yang efisien dapat dicapai apabila memenuhi keperluan penjajaran tenaga iaitu, $LUMO_{fluorofora}$ > potensi redoks elektrolit > $HOMO_{fluorofore}$. Kertas kerja ini membentangkan kajian kecekapan pengenerasian semula sel suria eksitonik yang dibentuk menggunakan tiga elektrolit berasaskan polimer iaitu, (i) 60% karboksimetil selulosa (CMC) yang dicampur dengan 40% alkohol polivinil (PVA), (ii) *alginate* dan (iii) *xanthan*. Potensi redoks elektrolit (E_o) dihitung menggunakan pengiraan kimia kuantum di bawah rangka *density functional theory* (DFT). Analisis fluorofora dan elektrolit adalah sesuai berdasarkan kepada penjajaran tahap tenaga. Setiap sel yang dibina dengan menggunakan tiga jenis elektrolit telah dianalisis; CMC/PVA menghasilkan kecekapan tertinggi, 1.39% di bawah pencahayaan yang bersamaan dengan satu Matahari. Nilai keberkesanan setiap sel adalah rendah kerana E_o elektrolit tidak bersesuaian kerana menunjukkan tahap tenaga yang lebih tinggi daripada $LUMO_{fluorophora}$. Sel berasaskan *alginate* dan *xanthan* menunjukkan sifat photovoltaik yang lebih rendah (iaitu, voltan litar terbuka, arus litar pintas, faktor pengisi dan) daripada sel berasaskan CMC/PVA. Hipotesis daripada pemerhatian tersebut adalah kerana penambahan tenaga di antara E_o dan $HOMO_{fluorophora}$.

Keywords: alginate, cmc/pva, dft, efficient electron regeneration, redox potential, xanthan

1. Introduction

Electron regeneration in the highest occupied molecular orbital of fluorophore ($HOMO_{fluorophore}$) is a crucial process that ensures a complete photovoltaic (PV) cycle. A complete device structure and an ideal working mechanism of an excitonic solar cell are illustrated in Figure 1(a) and 1(b), respectively. The main components of the excitonic solar cell are the (i) fluorophore, (ii) photoelectrode, and (iii) electrolyte, which function as the medium for electron excitation, transportation, and regeneration, respectively [1–3]. The fluorophore acts as a light absorber, which excites an electron from the $HOMO_{fluorophore}$ to the lowest unoccupied molecular orbital of fluorophore ($LUMO_{fluorophore}$) upon absorption of photon with sufficient energy (E_{photon} > bandgap, $E_{g\text{-}fluorophore}$). A vacancy (hole) is formed in the $HOMO_{fluorophore}$ during this stage [4]. Subsequently, the excited electron undergoes an injection process from $LUMO_{fluorophore}$ to $LUMO_{photoelectrode}$. A typical photoelectrode used in the excitonic solar cell is TiO_2, which functions as a medium for the transportation of the excited-state electron to the external circuit.

The electron vacancy in the $HOMO_{fluorophore}$ could be replenished using electrolyte during the electron regeneration mechanism. Therefore, E_o is highlighted as the key toward an efficient regeneration process; thus, the requirements of $LUMO_{fluorophore} > E_o > HOMO_{fluorophore}$ should be fulfilled [5–8]. The redox process, which occurs in the electrolytes, involves (i) reduction (the electron is received from the external circuit to the electrolyte) and (ii) oxidation (the electron is injected from the electrolyte to the fluorophore). However, this study focused on the oxidation potential of the electrolytes, which is closely related to the regeneration process.

Quantum chemical calculations under the density functional theory (DFT) framework could be used to calculate E_o of the polymer-based electrolyte with high accuracy [9–12]. The standard calculations could be performed in three main stages, i.e., (i) geometrical optimization of the oxidized and reduced states of electrolytes (in the gas and solvated phases), (ii) calculations of the Gibbs free energies in the gas and solvated phases, and (iii) calculations of the redox potential. The stated polymer-based electrolytes are preferred because of three factors, i.e., (i) considerable attention focused on biodegradable polymer electrolytes because of their application in electrochemical devices, including solar cells; (ii) low cost and abundance of natural polymers; and (iii) optimum ionic conductivity of polymer electrolytes, i.e., $\sigma_{CMC/PVA} = 7.93 \times 10^{-5}$ S/cm [13], $\sigma_{alginate} = 10^{-6}$ S/cm, and $\sigma_{xanthan} = 9.12 \times 10^{-6}$ S/cm [14].

Furthermore, the experimental and theoretical values of the redox potential of the electrolytes have not been established. Therefore, this study further investigated the detrimental effect on electron regeneration, which is hypothesized to be rooted from an offset between E_o and $HOMO_{fluorophore}$.

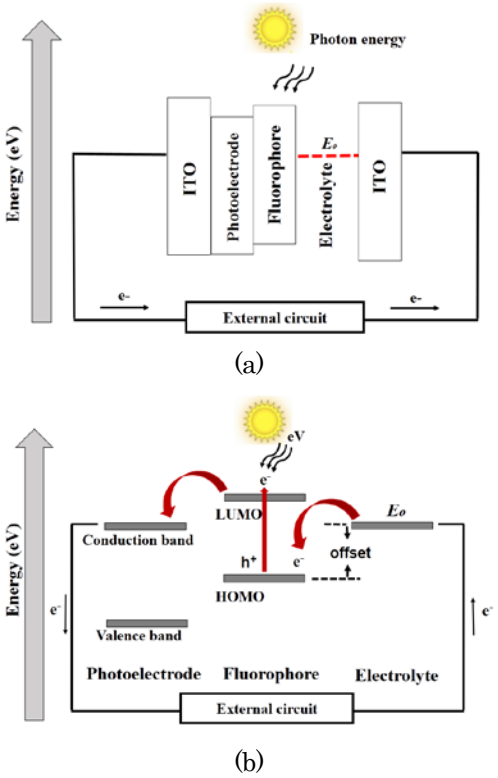

Figure 1. (a) Device Structure and (b) Working Mechanism of an Excitonic Solar Cell

2. Experimental

Materials. Materials used in the experiment were xanthan powder (Sigma Aldrich), carboxymethyl cellulose (CMC), polyvinyl alcohol (PVA), alginate powder (Sigma Aldrich), lead (II) sulfide (Sigma Aldrich; 99.9%), nitric acid (American Chemical Society reagent; 37%), titanium dioxide (R&M Chemicals), absolute ethanol (Merck; 99.5%), and indium tin oxide (ITO; Sigma Aldrich), with the following properties: (i) size of 0.7 mm (height), 355 mm (width), and 406 mm (length), (ii) thickness of 150 ± 20 nm, (iii) sheet resistance of 8 Ω/sq, and (iv) transmittance of 80%.

Sample Preparations. The working electrode of the solar cells was prepared using the following techniques. Titanium dioxide paste was prepared by dissolving 1.5 g TiO_2 powder in 1 mL concentrated nitric acid and 2 mL ethanol. The photoelectrode layer (TiO_2) was fabricated using stencil printing technique on an active area of 1 cm × 1 cm and heated at 100 °C for 10 min. The lead sulfide (0.24 g) layer was fabricated on the TiO_2 layer using a thermal evaporator (Magna Value Thermal Evaporator) in an environment with pressure, potential,

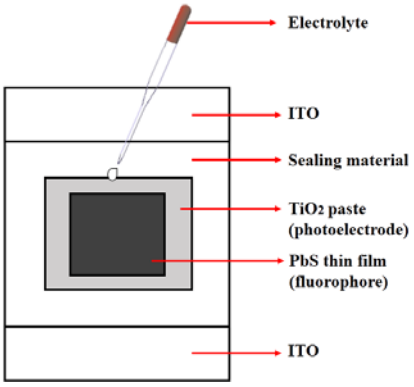

Figure 2. Schematic Diagram of a Solar Cell Fabricated Using Polymer-based Electrolytes

and current of 1.5 × 10^{-3} Torr, 1.53 V, and 65 A, respectively, to obtain good adsorption of the fluorophore (PbS) on the photoelectrode. The schematic diagram of the fabricated solar cell using polymer-based electrolytes is illustrated in Figure 2. Three polymer-based electrolytes were prepared in this work. The polymer-based electrolyte was made by dissolving 2.0 g CMC/PVA in 100 mL distilled water. The mixture was continuously stirred for approximately 24 h to form a homogenous solution. The alginate- and xanthan-based polymer electrolytes were prepared by dissolving 2.0 g alginate and xanthan powder, respectively, in 100 mL distilled water using the same procedure. A working solar cell was completed by layering a few drops of the polymer-based electrolytes in between a working electrode and a blank ITO.

Realistic Electrolyte Modelling. The structure of the electrolytes was optimized to the lowest energy structure through quantum chemical calculations conducted using the Gaussian 09W software package at the b3lyp/lanl2dz level of theory [15]. The models were evaluated and established as realistic using harmonic frequency calculations, thereby obtaining positive frequencies. Models with negative frequencies were discarded because of the nonrealistic vibrational mode. The ground- and excited-state energy levels of the realistic clusters were calculated using time-dependent DFT. The standard one-electron redox potential of the three polymer electrolytes was calculated by simulating negatively charged, positively charged, and neutral-state molecules of electrolytes to mimic the reduction and oxidation processes [16–20]. Numerous methods have been established to calculate the E_o potentials of electrolytes [21–23].

In this study, the Born–Haber cycle was used to calculate E_o, which utilized six parameters, i.e., (i) enthalpy of electron attachment in the gas phase (E_{SCF} $I_{(gas)}$), (ii) free energy of electron attachment in the gas phase (G $I_{(gas)}$), (iii) Gibbs energy thermal correction in the gas phase (G_{corr}), (iv) difference of solvent free energy (ΔG $I_{(solv)}$), (v) enthalpy of electron attachment in the solvent phase (E_{SCF} $I_{(solv)}$), and (vi) free energy of electron attachment in the solvent phase (G $I_{(solv)}$). The negatively charged (anion-state) models of the electrolyte were selected upon convergence of the requirements of the calculations, i.e., maximum force (0.00045 Hartree/Bohr), root mean square force (0.00030 Hartree/Bohr), maximum displacement (0.00180 Bohr), and root mean square displacement (0.00120 Bohr). The positively charged (cation-state) models were discarded because of convergence failure, which resulted in nonrealistic models. E_{SCF} I(gas) and G_{Corr} were obtained from geometry optimization and harmonic frequency calculations in the gas phase, respectively. The E_{SCF} I(*solv*) energy value was obtained from energy calculations in solvent (water). G I(gas), G I(solv), and ΔG (solv) I was calculated using the following equations, respectively:

$$G\ \mathrm{I(gas)} = E_{SCF}\ \mathrm{I(gas)} + G_{Corr} \quad (1)$$

$$G\ \mathrm{I(solv)} = E_{SCF}\ \mathrm{I(solv)} + G_{Corr} \quad (2)$$

$$\Delta G\ \mathrm{(solv)\ I} = E_{SCF}\ \mathrm{I(solv)} - E_{SCF}\ \mathrm{I(gas)} \quad (3)$$

The calculations of E_{SCF} II(gas), G_{corr}, E_{SCF} II(solv), G II(gas), G II(solv), and ΔG (solv) II in the neutral state were obtained using the same procedure. The difference in the solvation phase free energy of the electron in the anion and neutral states, ΔG_{ox}(solv), was calculated using the following equation:

$$G\ I(gas) = E_{SCF}\ I(gas) + G_{Corr} \quad (4)$$

The standard one-electron redox potential, E_o, was calculated using the following equation:

$$E_0 = \frac{\Delta G_{OX}\ (solv)}{-F} \quad (5)$$

where F is the Faraday constant (23.06 kcal/mol V), yielding a value of −2.013770507 V vs standard hydrogen electrode equivalent to −2.42623 eV vs vacuum.

3. Results and Discussion

Energy Level Alignment Analysis. The calculated energy levels of the redox potentials of polymer electrolytes, HOMO and LUMO of fluorophore, and photoelectrode are presented in Figure 3(a) to 3(c). The established report has showed that the minimum conduction band (-4.1 eV) and maximum valence band (-7.2 eV) energies of TiO_2 (photoelectrode) [24].

Notably, the excited-state electron could be injected efficiently from the $LUMO_{PbS}$ to the $LUMO_{TiO2}$ because of the fulfillment of the requirements of $LUMO_{PbS}$ (−4.0 eV) > $LUMO_{TiO2}$ (−4.1 eV). Energy loss is expected to be minimal, i.e., approximately 0.1 eV, during the injection process.

Despite the efficient injection, efficient electron regeneration from the electrolytes to the $HOMO_{PbS}$ was inhibited because the value of E_o of the electrolytes is higher than that of $LUMO_{PbS}$ and $HOMO_{PbS}$, i.e., $E_{o\ xanthan}$ (−1.605 eV) > $E_{o\ alginate}$ (−1.908 eV) > $E_{o\ CMC/PVA}$ (−3.144 eV) > $LUMO_{PbS}$ (−4.0 eV) > $HOMO_{PbS}$ (−5.1 eV). Two detrimental factors could be inferred from energy level alignment analysis, i.e., (i) inefficient electron injection from E_o to $HOMO_{PbS}$ because of the large energy offset and (ii) unnecessary injection from $E_{o\ electrolytes}$ to $LUMO_{PbS}$. A large energy offset between E_o and $HOMO_{PbS}$ was observed, i.e., $offset_{CMC/PVA}$ (1.956 eV), $offset_{alginate}$ (3.192 eV), and $offset_{xanthan}$ (3.495 eV), which would promote the unnecessary injection from E_o to $LUMO_{PbS}$ [25, 26].

The calculated E_o was hypothesized to be unsuitable for alignment with PbS as it is unable to fulfill the requirements of $LUMO_{PbS}$ > E_o > $HOMO_{PbS}$ for an efficient electron regeneration. Therefore, further analysis or replacement of the fluorophore is needed.

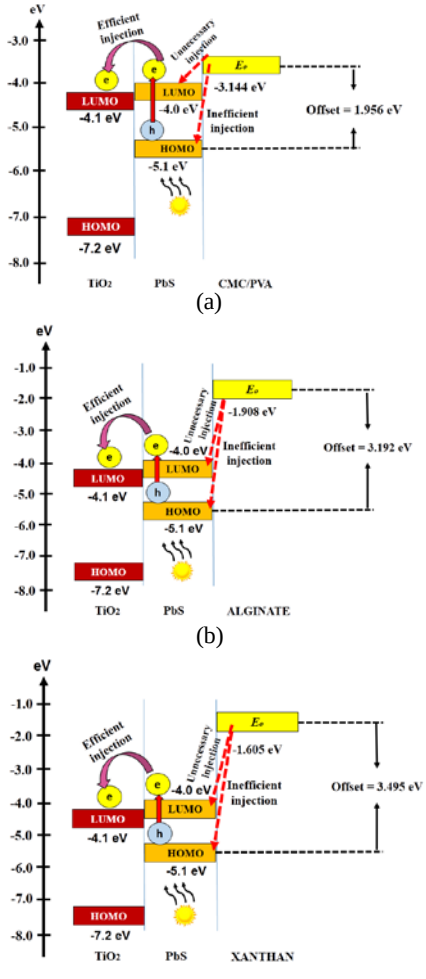

Figure 3. Energy Level Alignment of Solar Cells Fabricated using (a) CMC/PVA-based, (b) Alginate-based, and (c) Xanthan-based Electrolytes

Photovoltaic Studies. The PV parameters of the fabricated solar cells are shown in Figure 4. The calculated parameters of the CMC/PVA-based solar cell, i.e., η = 1.39%, open circuit voltage (V_{oc}) = 610 mV, short circuit current (I_{sc}) = 28.9 mA/m^2, maximum power (P_{max}) = 13.9 W/m^2, and fill factor (FF) = 28.9%, under the illumination of the sun, are indicated in Figure 4(a).

The calculated PV parameters of the alginate- and xanthan-based cells presented in Figure 4(b) and 4(c), respectively, yielded a low η. This finding can be attributed to the observation that electron regeneration is hindered by the high value of E_o, which promotes the two detrimental factors mentioned in the previous section [27].

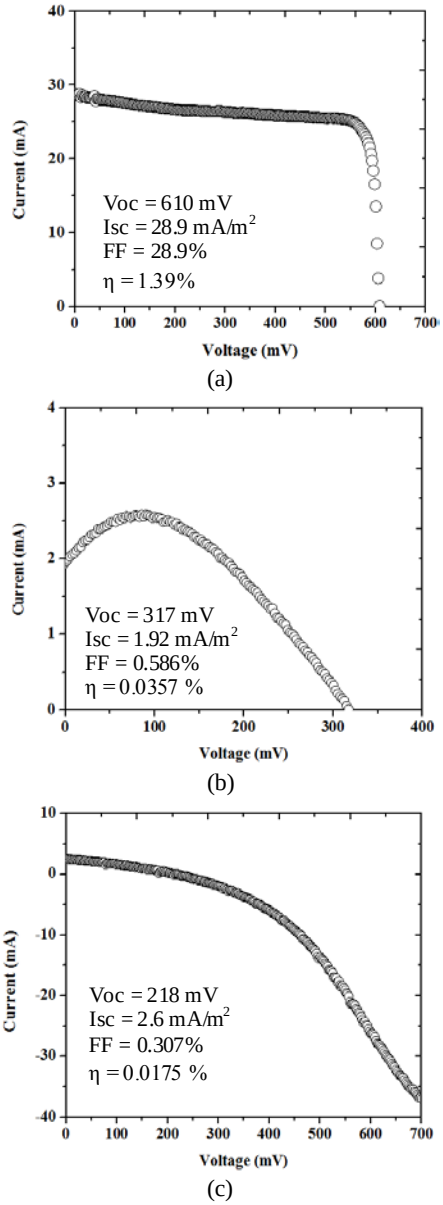

Figure 4. Current–Voltage Curves of Solar Cells Fabricated using (a) CMC/PVA-based, (b) Alginate-based, and (c) Xanthan-based Electrolytes

Structural Analysis. The optimized structure of polymer-based electrolytes is illustrated in Figure 5. The CMC/PVA, alginate, and xanthan molecules consist of three, one, and three carboxyl groups ($-COO^-$), respectively. The carboxyl group attached to the branch of the electrolytes was speculated to be able to increase the structural interaction. The CMC/PVA- and xanthan-based electrolytes are speculated to have more structural interaction than the alginate-based electrolyte. Therefore, the number of carboxyl groups in the electrolyte structure would increase the ion mobility during the interaction. The rate of ion mobility is directly proportional to the conductivity of electrolytes, enhancing the short circuit current, I_{sc}, which promotes the increment of η of the solar cell.

Therefore, electrolytes that yield a high-I_{sc} PbS/TiO_2-based solar cell could be speculated to be based on the number of carboxyl groups existing in the structure and the energy offset (discussed in the previous section). The performance of the electrolytes can be ranked (from high to low) as follows: CMC/PVA (three carboxyl groups, 1.956 eV offset), xanthan (three carboxyl groups, 3.495 eV offset), and alginate (one carboxyl group, 3.192 eV offset). Despite the remarkable findings on electrolytes, low η of the fabricated solar cells was reported. Low penetration of the polymer-based electrolytes into the mesopores of TiO_2, which can be attributed to the large radius size of the polymer chain compared with the pore size of the mesoporous TiO_2, is speculated to be the hindering factor [28–33].

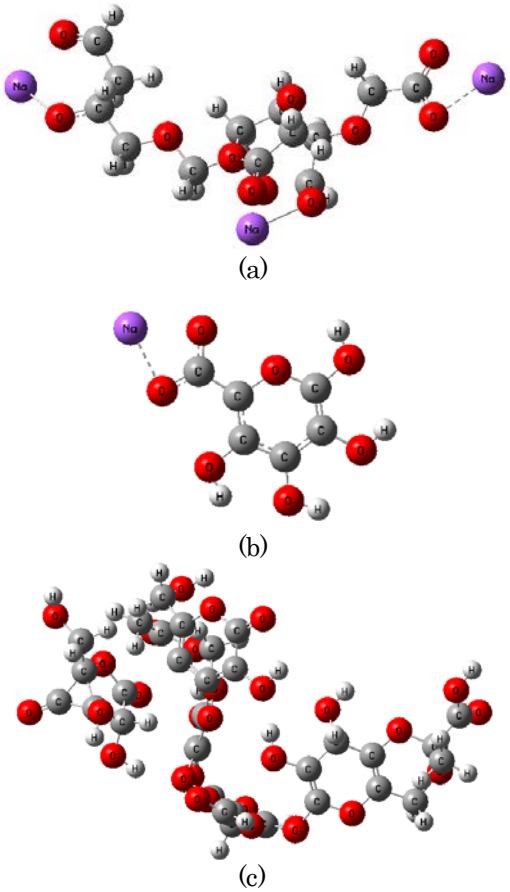

Figure 5. Optimized Structures of (a) CMC/PVA-based, (b) Alginate-based, and (c) Xanthan-based Electrolytes

4. Conclusions

The CMC/PVA-, alginate-, and xanthan-based electrolytes cannot be paired with PbS as fluorophore because the value of E_o is higher than that of $LUMO_{PbS}$ and $HOMO_{PbS}$. The stated energy alignment is unable to fulfill the requirements of an efficient electron regeneration, i.e., $LUMO_{fluorophore} > E_o > HOMO_{fluorophore}$, which would promote the unnecessary electron injection from the electrolytes to the $LUMO_{PbS}$. Furthermore, the energy offset between E_o and $HOMO_{PbS}$ is large, i.e., $offset_{CMC/PVA\text{-}PbS}$ = 1.956 eV, $offset_{alginate\text{-}PbS}$ = 3.192 eV, and $offset_{xanthan\text{-}PbS}$ = 3.495 eV, which would promote the unnecessary electron injection to the $LUMO_{PbS}$ and suppress the electron regeneration in the $HOMO_{PbS}$.

Acknowledgements

This work is funded by the Research & Innovation Department of Universiti Malaysia Pahang and the Ministry of Education of Malaysia through the Fundamental Research Grant Scheme (RDU 150111).

References

[1] D. Zhou, T. Zhou, Y. Tian, X. Zhu, Y. Tu, J. Nanomater. 2018 (2018) 1.
[2] N.A. Chuchvaga, D.V. Zhilina, S.R. Zhantuarov, S.Z. Tokmoldin, E.I. Terukov, J. Phys.: Conf. Ser. 993/1 (2018) 012039.
[3] A.A. Baloch, S.P. Aly, M.I. Hossain, F. El-Mellouhi, N. Tabet, F.H. Alharbi, Scientific Reports. 7/1 (2017) 11984.
[4] S. Bernacchi, Y. Mély, Nucleic Acids Res. 13 (2000) 29.
[5] W. Feng, A.S. Wan, E. Garfunkel, J. Phys. Chem. C. 19 (2003) 117.
[6] W. Feng, S. Rangan, Y. Cao, E. Galoppini, R.A. Bartynski, E. Garfunkel, J. Mater. Chem. 19 (2014) 2.
[7] D.P. Hagberg, T. Marinado, K.M. Karlsson, K. Nonomura, P. Qin, G. Boschloo, L. Sun, J. Org. Chem. 25 (2007) 72.
[8] H. Ishii, K. Sugiyama, E. Ito, K. Seki, Adv. Mater. 8 (1999) 11.
[9] P. Gu, D. Yang, X. Zhu, H. Sun, P. Wangyang, J. Li, H. Tian, AIP Advances. 7/10 (2017) 105219.
[10] M. Uudsemaa, T. Tamm, J. Phys. Chem. A. 46 (2003) 107.
[11] L. Goerigk, S. Grimme, Phys. Chem. Chem. Phys. 14 (2011) 13.

[12] L. Yan, Y. Lu, X. Li, Phys. Chem. Chem. Phys. 7 (2016) 18.
[13] Y.O. Iwaki, M.H. Escalona, Briones, A. Pawlicka, Mol. Cryst. Liq. Cryst. 554 (2012) 221.
[14] F.C. Tavares, D.S. Dörr, A. Pawlicka, C. Oropesa Avellaneda, J. App. Polym. Sci. 135 (2018) 46229.
[15] M.J. Frisch, G.W. Trucks, H.B. Schlegel, G.E. Scuseria, M.A. Robb, J.R. Cheeseman, G. Scalmani, V. Barone, B. Mennucci, G.A. Petersson, et al., Gaussian 09, R.A. 1, Gaussian. Inc., Wallingford CT. 121 (2009) 150.
[16] M.H. Baik, R.A. Friesner, J. Phys. Chem. A. 32 (2002) 106.
[17] L.E. Roy, E. Jakubikova, M.G. Guthrie, E.R. Batista, J. Phys. Chem. A. 24 (2009) 113.
[18] S. Rajamani, T. Ghosh, S. Garde, J. Chem. Phys. 9 (2004) 120.
[19] M.T. McDonnell, D.A. Greeley, K.M. Kit, & D.J. Keffer. J. Phys. Chem. B. 34 (2016) 120.
[20] S.K. Muzakir, Malaysia University Conference Engineering Technology, 2014. p. 79.
[21] M.Brandbyge, J.L. Mozos, P. Ordejón, J. Taylor, K. Stokbro, Phys. Rev. B. 16 (2002) 65.
[22] M. Liu, S.M. Han, X.W. Zheng, L.L. Han, T. Liu, Z.Y. Yu, Int. J. Electrochem. Sci. Belgrade. 10 (2015) 235.
[23] K. Arumugam, U. Becker, Miner. 4 (2014) 345.
[24] Z. Zhang, Y. Yu, P. Wang, ACS Appl. Mater. Interfaces. 4 (2002) 990.
[25] S.K. Kim, P. Ho, J.W. Lee, S.Y. Jeon, S. Thogiti, R. Cheruku, J.H. Kim, Mol. Cryst. Liq. Cryst. 1 (2017) 653.
[26] P. Peljo, H.H. Girault, Energy Environ. Sci. 11 (2018) 2306.
[27] S. K. Muzakir, N. Alias, M.M. Yusoff, R. Jose, Phys. Chem. Chem. Phys. 15 (2013) 16275.
[28] J. N. D. Freitas, A. F. Nogueira, M. A. Paoli, J. Mater. Chem. 19 (2009) 5279.
[29] J. Y. Kim, T. H. Kim, D. Y. Kim, N.G. Park, K.D. Ahn, Power Sources 175 (2008) 692.
[30] L. Jin, Z. Wu, T. Wei, J. Zhai, X. Zhang, Chem. Commun. 47 (2011) 997.
[31] Y. Wang, Sol. Energy Mater. Sol. Cells, 93 (2009) 1167.
[32] M.A. Saadiah, A.S. Samsudin, IOP Conf. Ser.: Mater. Sci. Eng. IOP Publishing. 342/1 (2018) 012045.
[33] H. Pujiarti, W.S. Arsyad, L. Muliani, R. Hidayat, J. Phys.: Conf. Ser. IOP Publishing. 1011/1 (2018) 012020.